Multi-Band Simulation of Interband Tunneling Devices Reflecting Realistic Band Structure

Matsuto Ogawa, Ryuichiro Tominaga, and Tanroku Miyoshi

Department of Electrical and Electronics Engineering
Kobe University, 1 Rokkodai, Nada, Kobe 657-8501, Japan
Phone & Facsimile: +81-78-803-6074
E-mail: ogawa@eedept.kobe-u.ac.jp

***Abstract*- We have studied quantum transport in a Si interband tunneling diode (ITD) based upon a tight-binding non-equilibrium Green's function method. In the simulation, an empirical tight-binding theory has been used to take into account realistic band structures. Comparison has been made between the results of our multiband (MB) model and those of conventional two-band (2B) model. It is found that the current-voltage (I-V) characteristics of the Si ITD have considerably smaller peak current density than the 2B model, since our MB model reflects the nature of indirect gap structure.**

I. Introduction

The speed of semiconductor device miniaturization has been accelerated in order to increase packing densities and reduce power consumption in integrated circuits (IC's). In particular, progress in Si MOSFETs technology has nowadays made it possible to reduce gate lengths down to less than 100 nm. However, at such small dimensions, conventional FETs suffer from inevitable limitations due to the emergence of quantum effects such as interband tunneling, current fluctuations, and gate-oxide tunneling. To overcome such limitations, devices based on tunneling mechanisms, such as interband tunneling diodes (ITD's), have been reconsidered as promising components for future circuit technologies, since tunneling occurs within a very small region. In addition, they have increased functionality due to the negative differential resistance, which can be used to reduce device numbers in IC's as well as avoid complex circuit design.

Although various devices have been demonstrated [1, 2], full understanding of the device physics is still necessary to design device structures and optimize the device performance. So far, only simple two-band model has been applied to analyze the characteristics of ITD's, but failed to reflect complex band structures of the materials. In order to simulate carrier transport in such devices realistically, we have to include properly the full band structure effect such as the band mixing between the conduction band and the valence band.

In this paper, we present calculations of quantum electron transport in a Si ITD based on a non-equilibrium Green's function formalism. In the next section, we describe a tight-binding Green's function method. In our procedure, we employ an empirical sp^3s^* nearest neighbor tight-binding (TB) model[3] and an evanescent-wave-mode-matching method to include the valley mixing and nonparabolicity effects, in addition, possible existence of evanescent modes at heterointerfaces[4, 5]. We show numerical results compared with those calculated by the conventional two band model for a Si ITD. Finally, we summarize our conclusion.

II. Simulation Model

The present model refers to a 1D Si n^+-p^+ ITD as schematically shown in Fig. 1. Our simulation approach of multiband quantum transport is based on a non-equilibrium Green's function method (NEGF) with an empirical tight-binding method. We confine ourselves to the analysis of carrier transport in the [0 0 1] direction in Si crystal. We use an empirical tight-binding model with a basis of five orbitals per atom (s, p_x, p_y, p_z, s^*) assuming nearest neighbor overlaps. The band structure of Si is then calculated where not

0-7803-6279-9/00/$10.00 © 2000 IEEE

only the propagating Bloch modes but also the existence of the decaying modes (evanescent ones) in the tunneling barrier are taken into account.

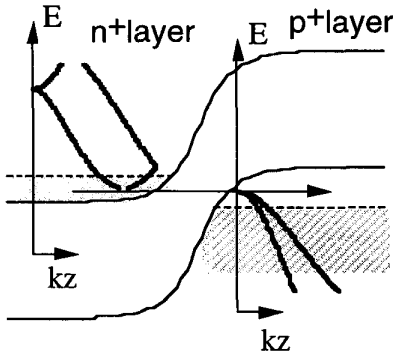

Fig. 1. Schematic structure of a Si interband tunneling diode (ITD). Two propagating modes exist in the conduction band, whereas three modes exist in the valence band because the heavy hole band is doubly degenerated (excluding spin degeneracy). Doping concentrations of $N_D = N_A = 1 \times 10^{20}$ cm^{-3} are assumed.

The total electron wave function may be expressed in terms of the Bloch sum of the electronic states as

$$|\Psi(k_z, \boldsymbol{k}_\parallel, z)\rangle = \sum_{l,\alpha^a,\alpha^c} \left[c_{l\alpha^a}(k_z)|\boldsymbol{k}_\parallel, l, \alpha^a\rangle + c_{l\alpha^c}(k_z)|\boldsymbol{k}_\parallel, l, \alpha^c\rangle\right], \quad (1)$$

where $|\boldsymbol{k}_\parallel, l, \alpha^j\rangle$ denotes a Bloch sum of α^j-like atomic orbitals associated with the in-plane wave vector $\boldsymbol{k}_\parallel$, k_z the wave vector in propagating direction, l labels the index of the layer comprised of an atom (a) and its nearest neighbor (c). We follow the treatment of the NEGF[6, 7, 8]. A propagator $G^<$ and a retarded Green's function G^R are comprised of the expansion coefficients in Eq.(1). The equations of motion for $G^<$ and G^R in the device are given with the aid of the Dyson's equation by

$$G^< = G^R \Sigma^{<B} G^{R\dagger}, \quad (2)$$

$$G^R = (E_z - H_0^D - \Sigma^{RB})^{-1}, \quad (3)$$

where $G^<$ *etc.* are matrices , $\Sigma^{<B}$ and Σ^{RB} are boundary self-energies, and H_0^D is the Hamiltonian of the device region, respectively. The boundary self-energies are related to TB parameters and boundary conditions in the reservoirs, where the existence of the evanescent modes can be duly taken into account[5, 9].

By solving the equations of motion with respect to $G^<(\boldsymbol{k}_\parallel, E_z)$, we can calculate both the electron concentration and the current density at layer L as follows,

$$n_L = -\frac{2i}{A\Delta} \sum_{\boldsymbol{k}_\parallel} \int \frac{dE_z}{2\pi} \mathbf{Tr}\left[G^<_{L,L}(\boldsymbol{k}_\parallel, E_z)\right], \quad (4)$$

$$J_L = \frac{2e}{\hbar A} \sum_{\boldsymbol{k}_\parallel} \int \frac{dE}{2\pi} 2\mathbf{Re}\left\{\mathbf{Tr}\left[-t_{L,L+1} \cdot G^<_{L+1,L}(\boldsymbol{k}_\parallel, E_z)\right]\right\}, \quad (5)$$

where A is the cross sectional area, Δ is a half of the lattice constant, e the electronic charge, $t_{L,L+1}$ is the *hopping matrix* which is related to the matrix elements of the Hamiltonian, **Tr** denotes trace of the matrix, and **Re** is real part of the physical quantity. Poisson's equation

$$\frac{d}{dz}\left[\epsilon(z)\frac{d\phi(z)}{dz}\right] = e\left[n(z) - N_D(z) + N_A(z)\right], \quad (6)$$

is simultaneously solved to include the space charge effect for selfconsistent calculation, where ϵ is the dielectric constant and N_D is the donor and N_A is the acceptor doping concentration, respectively.

The TB and material parameters used in the simulation is extracted from the literature[3].

III. Results and Discussion

Figure 2 shows a comparison of the band structures of Si crystal calculated by the conventional two band (2B) model and the multi-band (MB) model. Imaginary wave vectors are plotted on the left, which correspond to decay constants, whereas real wave vectors corresponding to the Bloch modes are plotted on the right.

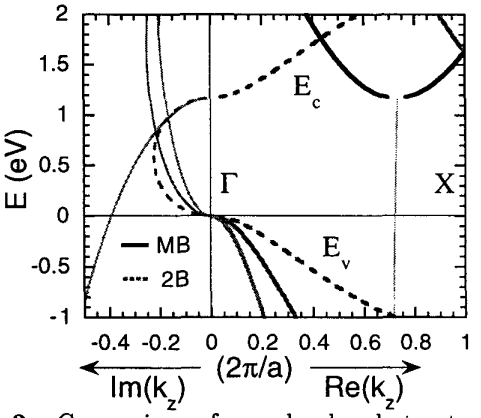

Fig. 2. Comparison of complex band structures of Si calculated by the MB (solid lines) and the 2B model (dashed lines). The real bands ($\mathbf{Re}k_z$) are drawn on the right portion, whereas the imaginary bands ($\mathbf{Im}k_z$) are on the left.

The evanescent modes as well as the real bands should be considered at a tunneling interface to match electron waves, since a disruption of translational symmetry occurs at the interface.

It is found that although the effective mass in the conduction band is approximated by the 2B model, the imaginary bands and, more importantly, the position of the conduction band minimum cannot be reproduced by the 2B model. When we fit the electron effective mass to the actual data, the hole effective mass is automatically set equal to that of the electron in the 2B model, which is also far from the reality. On the other hand, the nearest neighbor MB model seems to approximate relatively well the indirect gap structure of Si in the [0 0 1] direction.

To verify the difference of the band structure models in the device characteristics of the Si ITD, we compare the I-V characteristics of the MB model (Fig.3 (a)) with those calculated by the 2B model (Fig.3(b)).

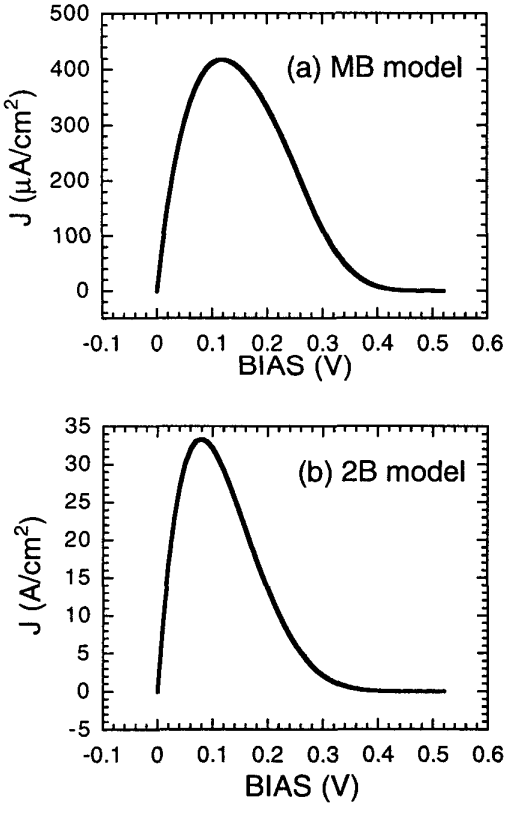

Fig. 3. (a)I-V characteristics of the Si ITD calculated by the multiband (MB) model. (b)I-V characteristics calculated by the two-band (2B) model .

It is found that the peak current density of the MB model is considerably smaller than that of the 2B model. To understand the difference between the two band models, we show the transmission state in Fig. 4 (a) and (b) for the MB and 2B model, respectively. The element of the spectral function $A_{N,1}(= i(G^R - G^{R\dagger})_{N,1})$ corresponds to the transmission probability. Since the 2B model assumes the band extremes exist at the Γ valley, electron in the s-state in the n^+ region tunnels and couples that in the p_z-state in the p^+ region (Fig.4(b)). However, in the MB model, the contribution of the s^* orbital to the X band minimum is so large that tunneling components through other orbitals compete one another. As a result, as shown in Fig. 4(a), the s^*, s, and p_z electrons are affected with more decay and have smaller tunneling probability. Consequently the MB model has smaller current density, which reflects the indirect gap structure of Si.

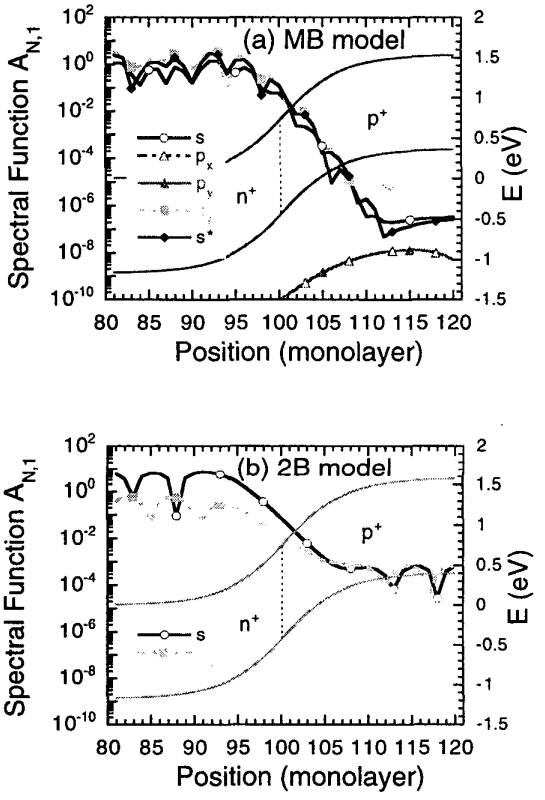

Fig. 4. (a)Spectral function or transmission amplitude calculated by the multiband (MB) model. The s^*-component as well as the s and p_z are found to be dominant in the conduction band. (b)Spectral function by the 2B model. Since both the conduction and the valence bands are assumed to be comprised of the s and p_z-like atomic orbitals, the spectral function is larger than that in the MB model.

The significant difference of the order of 5 in the peak current densities may be due to the TB parameterization [3], where the coupling of the s^* orbital with the neighboring s states is neglected. Figure 5 shows the constant energy surface of Si in the first Brillouin zone calculated by the nearest neighbor MB model. This figure does not show the 6 rotated ellipsoids seen in the conventional *ab initio* band calculations. This fact indicates that the nearest neighbor sp^3s* model does not sufficiently express the properties of X minima of Si crystal. That is the reason we have obtained considerably smaller current density in the MB model although we have taken into account the realistic band structures. To analyze quantum transport in Si crystal more quantitatively, we may have to approximate the band structure more accurately by taking into account higher (*e.g.* 2nd nearest neighbor) interactions among sp^3s* orbitals.

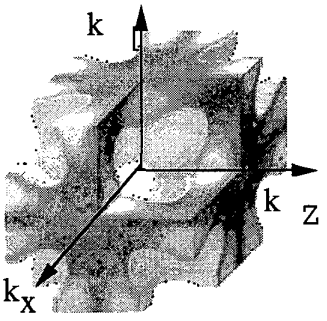

Fig. 5. Constant energy surface ($1.2 \leq E \leq 1.6$ eV: X minima) of Si calculated by the nearest neighbor interaction sp^3s* model. The 1-st quadrant is cut out to show inside.

IV. Cnclusion

We have studied multiband quantum transport in a Si ITD based on the tight-binding non-equilibrium Green's functions, where full-band nature of realistic band structures and space charge effect are taken into account. It is found the conventional 2B model cannot analyze the interband tunneling, since the 2B model cannot produce the indirect gap structure. On the other hand, the MB model can treat properly the interband tunneling process in the indirect gap material. It is also found that the transmissivity of the X-Γ interband tunneling is considerably small. This is due to the fact that the nearest neighbor approximation is insufficient to express the properties of X minima in Si crystal. More accurate tight-binding parameterization is needed for more quantitative analysis of the inter band tunneling in indirect gap semiconductors.

Acknoledgment

M.O. would like to thank Drs. G. Klimeck in JPL Cal. Tech. and M.P. Anantram in NASA ARC for their discussion.

References

[1] J. Koga and A. Toriumi, "Negative Differential Conductance in Three-Terminal Silicon Tunneling Device," Appl. Phys. Lett. **69**, pp.1435–1437, 1996.

[2] T. Baba and T. Uemura, "First Demonstration of A Planar-Type Surface Tunnel Transistor (STT): Lateral Interband Tunnel Device," Solid-St. Electron. **40**, pp.519–522, 1996.

[3] P. Vogl, H.P. Hjalmarson, and H.D. Dow, "A Semi-Empirical Tight-Binding Theory of the Electronic Structure of Semiconductors," J. Phys. Chem. Solids, **44**, pp.365–378, 1983.

[4] V. Heine, "On the General Theory of Surface States and Scattering of Electrons in Solids," Proc. Phys. Soc. **81** pp.300–310, 1960.

[5] M. Ogawa, T. Sugano, and T. Miyoshi, "Multiband Quantum Transport with Γ-X Valley-Mixing via Evanescent States," Solid St. Electron. **42**, pp.1527–1532, 1998.

[6] C. Caroli, R. Combescot, P. Nozieres, and D. Saint-James, "Direct Calculation of the Tunneling Current," J. Phys. C: Solid St. Phys. **4**, pp. 916–929, 1971.

[7] F. Sols, M. Macucci, U. Ravaioli, and K. Hess, "Theory for a Quantum Modulated Transistor," J. Appl. Phys. **66**, pp. 3892–3906, 1989.

[8] R. Lake, G. Klimeck, R.C. Bowen, and D. Jovanovic, "Single and Multiband Modeling of Quantum Electron Transport through Layered Semiconductor Devices," J. Appl. Phys. **81**, pp.7845–7869, 1997.

[9] M. Ogawa, T. Sugano, and T. Miyoshi, "Multiband Modeling of Quantum Electron Transport Based on the Green Function Theory," *Inst. Phys. Conf. Ser.* **162**, ed. H. Sakaki, pp.319–324, 1999.